Tribol Lett (2017) 65:133
DOI 10.1007/s11249-017-0916-7

ORIGINAL PAPER

Characteristics of Dummy Skin Contact Mechanics During Developing Process of Skin Abrasion Trauma

Xuewei Mao[1] · Yoji Yamada[1] · Yasuhiro Akiyama[1] · Shogo Okamoto[1]

Received: 18 May 2017 / Accepted: 22 August 2017

Abstract This study focuses mainly on potential skin abrasion risks that are likely to be caused by the interactive force on a contact surface between a human body and a physical assistant robot's cuff, particularly when these robots are misused. In this study, we develop a novel method for evaluating skin contact states in order to estimate abrasion risks. First, a simplified cuff model is designed to conduct abrasion tests on a piece of dummy skin. The skin is pasted onto a dummy's leg to simulate the human skin's viscoelastic properties. Then, the edge condition of the contact surface is measured while the cuff model slides on the dummy skin. We conduct an analysis of the interactive force and displacement between the cuff model and dummy skin and several principal influential factors are examined during the evolution of abrasion-induced skin damage. These results are applied to evaluate the contact conditions between the robot's cuff and human skin, which makes a significant contribution to estimating the risk of abrasion injuries for a physical assistant robot user.

Keywords Contact mechanics · Biotribology · Safety · Wear mechanism

This work was supported by AMED (Japan Agency for Medical Research and Development).

✉ Xuewei Mao
xueweimaomao@gmail.com

[1] Academy for Safety Intelligence, Department of Mechanical Science and Engineering, Graduate School of Engineering, Nagoya University, Furo-cho, Chikusaku, Nagoya 464-8603, Japan

1 Introduction

Skin surface abrasion damage is typically caused by an encounter with an abrasive surface [1]. Although it appears as relatively slight skin damage, abrasion trauma is usually more painful and unbearable than a deeper cut, as a result of the millions of nerve endings that are exposed without skin protection [2]. For example, it was reported that self-healing took more than twelve weeks in the case of a hip scratch test, which was considered well tolerated [3]. For the safe utilization of physical assistant robots, it is necessary to design the cuff part of the robot to prevent users from suffering abrasion traumas.

Stress concentration around the edge of a robot fixation cuff is considered to be the primary cause of skin abrasion trauma [4, 5]. The mechanism of scratch-induced damage to viscoelastic material has been investigated in various manners [6, 7], such as the evolution map [6] or scratch resistance [8]. It is widely accepted that the stress concentration around the scratching tip and pileup substrate are essential contributing factors to the development of scratch damage [6, 9]. Therefore, particular attention has been paid to stress concentration, to clarify the human skin abrasion damage process. However, few studies focusing on abrasion trauma have been conducted on the human body directly, because this involves inflicting abrasion suffering on human subjects [3].

To avoid the ethical controversy of human abrasion tests, Jee et al. [10] performed an in vitro investigation of shearing damage on porcine skin, and demonstrate how the normal load, scratching speed, and number of scratch cycles influence the skin sample friction coefficient. However, neither the external load nor scratch time on the microscale examined by Jee et al. is useful for providing information that enables us to establish practical safety

Published online: 02 September 2017

guidance for physical assistant robot use, which instead requires analysis of the macroscopic human–robot contact mechanics. Furthermore, it is crucial to utilize experimental subjects with relatively stable abrasion-induced damage characteristics, so that appropriate criteria can be determined efficiently during abrasion tests to develop a reliable method for evaluating human–robot contact states. This is evident based on the fact that the results of in vitro or in vivo tests on skin friction injuries were observed to vary with experimental subject individualities [11, 12].

In a previous study on blistering, which is another type of skin friction trauma, Xing et al. [13] reduced the disturbances of subject individualities by using a dynamic nonlinear finite-element model to replicate the skin structure. It is difficult for such a computer model to obtain detailed information, such as the effects of repeated abrasion on the skin surface during the abrasion injury development. However, variations in skin properties and the gradually increasing degree of abrasion damage play an important role in establishing an estimation method for robot user abrasion risks. Guerra et al. developed a synthetic skin simulant platform to investigate the mechanics of skin friction blisters and the effect of different surface treatments on the skin damage [14, 15], and Chimata et al. [16] further improved the skin simulant to a two-layer elastomeric model for investigating the influences of the normal load on the skin blister generation. Instead of simulation by computer, this human skin substitute was utilized to exhibit skin friction damage after a certain number of reciprocating cycles [14, 16]. Although there are an insufficient number of studies in terms of the contact mechanics, it can be concluded from previous blister studies that variations in skin mechanical properties may be observed during the development of abrasion-induced damage on a synthetic skin simulant [14, 16].

For our study, we selected a distinctive type of manufactured multilayer skin [17] as a substitute for an in vivo human skin subject. As exhibited in Tang et al.'s study [19], the near-surface deformation under scratches of polypropylene blends was similar to that of porcine skin specimens observed in previous in vitro tests [10]. Because the dummy skin applied in our study was also composed of polymers, it is considered to be feasible to substitute the skin samples under abrasion. The dummy skin properties showed hardly any individuality variations, and a wrinkle with a certain length value was invariably observed after the dummy skin was damaged by repetitive abrasion motions. In comparison with the previously tested human or animal materials [11, 12], our experimental subject provided a more stable abrasion damage degree criterion. Moreover, the dummy skin and human skin exhibit similarities in terms of the friction coefficient [17, 18], which is a critical property for human friction injury [20, 21], as well as viscoelasticity [17], which has a significant influence on human skin friction deformation components [22, 23]. For the abrasion motion on the dummy skin surface, a cuff model equipped with a group of force sensors was controlled by a manipulator and repeated unidirectional abrasion was conducted along a preset route. During the repetitive abrasion motion, cuff–skin contact surface friction behavior was monitored, and a significant clue of irreversible abrasion damage was observed by analyzing the decreasing tendency of the friction coefficient. As explained in the previous in vitro study [12], it was nearly impossible to obtain an invariable initial skin friction damage time point effectively by using porcine skin. However, if it can be verified that the development process of skin damage can be indirectly obtained by observing the varying tendency of the contact mechanics, the major obstacle of using porcine skin as a substitute will be removed. Our skin simulant can then be utilized for performing a reliable safety validation test after matching its characteristics to those of porcine skin.

According to previous studies on scratch-induced damages on polymer, the indenter size [7, 8], tip velocity [7], specimen mechanical properties [7, 8], and external loads [6–8] have a significant effect on the severity of the damage. However, only the external load, abrasion velocity, and interaction frequency are noticeably affected by different usage of physical assistant robots. Therefore, in our study, we mainly focused on these three physical parameters and compared their influences on the abrasion damage development process on the dummy skin. Although the abrasion times were rarely mentioned in the conventional mechanical model of abrasion-induced damage, considering the possibility of applying our study in the practical robot use, the number of abrasion times was chosen as a criterion in the establishment of an analytical model for the abrasion damage mechanism regarding the cuff–skin contact state.

In this study, we developed an experimental method for evaluating robot cuff–human skin contact states. The remainder of this paper is organized as follows. Section 2 provides a description of the entire experimental setup and describes the main features of the dummy skin and robot cuff model. In Sect. 3, the abrasion motion and adhesion test method used in the experiments are presented, followed by an explanation of all of the tested cuff–skin contact states. Section 4 introduces the unique characteristics of abrasion damage on the dummy skin surface and summarizes the variation principle of the mechanical properties during the abrasion damage development. The abrasion times' effects on the adhesion of dummy skin superficial layer were exhibited, and the varying tribological properties were also analyzed under different abrasion conditions. By comparing the influences of different

physical parameters on the abrasion damage development, our evaluation method for the contact states is verified to be feasible for making a considerable contribution to estimating the potential severity of skin abrasion trauma during physical assistant robot use.

2 Experimental Setup

2.1 Experimental Material

In order to gain high repeatability of an evaluation method, the properties of the experimental subject are required to be relatively stable. For this reason, we selected a special kind of dummy skin created in our laboratory [17] to substitute in vivo skin samples in this study. The main material types and structure of the dummy skin are shown in Fig. 1. The dummy skin's properties are similar to that of human skin, particularly in terms of viscoelasticity and the friction coefficient, which play an important role in the abrasion damage process. The thickness of the dummy skin's superficial layer is approximately 30 μm. This value is roughly equal to the total thickness of the stratum corneum and upper layers of epidermis [24], which typically constitute the part that is damaged during a skin scratch injury [25, 26]. According to Jee et al.'s scratch study [10], the superficial layer is first separated from the layer underneath during the initial skin scratch damage stage. Because the superficial layer may also first be separated from the bottom gel of the dummy skin when it is damaged by abrasion motions, the dummy skin is regarded as an appropriate substitute for human skin in the abrasion test.

2.2 Simplified Cuff Model

Due to the viscoelasticity and the variability of geometrical profile of human skin, the actual contact condition between the cuff of a physical assistant robot and human body is too complex to be evaluated directly. It is therefore necessary to design a simplified cuff model to simulate the contact condition and make it easier to monitor the interaction change between the cuff model and skin.

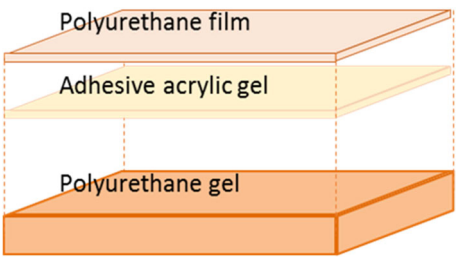

Fig. 1 Main material type and structure of dummy skin

Taking both the general shape and softness of the robot's cuff into consideration, the cuff model is designed as a flat punch with a rounded edge. Several force sensors were fixed to the cuff model in order to achieve cuff–skin interaction monitoring.

2.3 Main Experimental Apparatus

During the abrasion tests, the cuff model was moved by a manipulator (MOTOMAN-MH3F, Yaskawa Electric Corporation, Japan) on a dummy thigh model with a piece of dummy skin, which was composed of a human-skin-gel-sheet (H0-10, EXSEAL, Co., Japan) and film dressing tape (H24R10, Nitoms, Inc., Japan), pasted onto it. The cuff model was connected to the manipulator's end-effector, with a 6-axis force-moment sensor (IFS-67M25A50-140-ANA, NITTA, Japan) between the two. Figure 2 shows the main experimental apparatus. The cuff model consisted of a small fixing box, and sensor box base and surface (made with a uPrint SE Plus 3D Printer, Stratasys Ltd., and using ABSP430 XL model (black) as printing material). The components were assembled in the order shown in Fig. 3, from left to right.

2.4 Sensors for Monitoring Cuff–Skin Interaction

According to Giannakopoulos's study [9] on stress concentration caused by a rounded flat punch similar to our cuff model, the contact surface edge is the most hazardous area when the cuff conducts abrasion on the skin. Therefore, we focus mainly on the edge of the cuff model, which

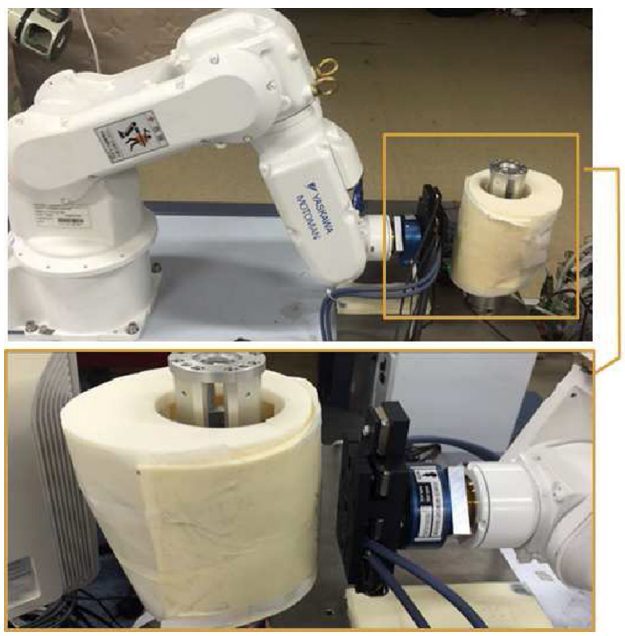

Fig. 2 Main experimental apparatus of abrasion test

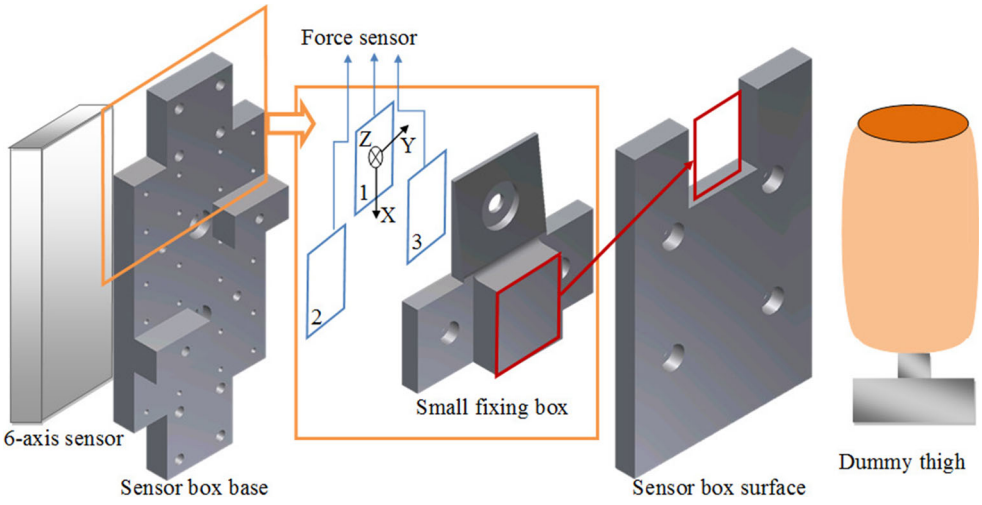

Fig. 3 Main components of sensor box and relative positions

is the small fixing box shown in Fig. 3. Three 3-axis force sensors (one USL06-H5-500N-C and two USL08-H6-1KN-C, Tec Gihan, Japan) were fixed onto the sensor box base with the small fixing box. Since the upper edge of the small fixing box will first make contact with the dummy skin and then conduct abrasion the skin during the test, it is necessary to ensure its size accuracy. Therefore, this small fixing box was manufactured with aluminum, and its rounded edge radius was measured using an industrial microscope (OLS4100, Olympus Corp., Japan).

The other parts of the sensor box are mainly for balancing the force and torques that may be generated when the entire sensor box contacts the dummy skin, so that we can obtain the interactive force on the edge in a real sense. The relative positions between these sensors and the sensor box base are shown in Fig. 3.

3 Experimental Design

3.1 Experimental Method

During the abrasion test, the manipulator end tip, equipped with the cuff model, was first moved to the bottom of the dummy leg, then conducts abrasion on the skin surface from the bottom to the top, and finally left the dummy skin. This motion is referred to as one abrasion time. Within one trial, the abrasion motion was repeated a preset number of times, such as one, two, or four. Between trials, the appearance of the skin surface was observed and a picture taken. The trial was repeated in one test until a stable phenotype was found on the dummy skin surface. Crucial phynotypes showing the gradually increasing abrasion damage severity were repetitively tested and, respectively, examined using field emission scanning electron microscopy (FESEM) (SPG-724, JEOL Ltd., Japan). The microscope was operated at an accelerating voltage of 5 kV.

In addition, the adhesion force of the dummy skin samples after three, five, and eight times of abrasion was also examined by a tension and compression testing machine (SV-52NA, IMADA SEISAKUSHO CO., LTD, Japan). Before the adhesion test, the sample width was cut into 10 mm which contains the main damaged area, and the superficial film was pre-peeled from one end of the sample strip, until it was less than 5 mm from the damaged area. Then, the pre-peeled end was fixed and lifted by the head part of the machine at a speed of 20 mm/min. The entire superficial layer was continued to be peeled while the peeling force and displacement of the fixing head were recorded simultaneously.

3.2 Experimental Condition

Because human skin viscoelasticity can be simulated using polymer materials, studies focusing on scratch-induced damage to polymers were included as important references when we decided on the parameters to be examined in the evaluation of contact states. In their study on scratch-induced polymer damage, Jiang et al. [6] claimed that the von Mises stress or normal load was directly related to the severity of damage. For a rounded punch, the maximum tensile stress around the cuff edge is mainly determined by the normal and tangential loads [9]. In addition, the edge radius and specimen thickness may affect the maximum stress calculation method [9]. "Scratch hardness," which is the most commonly used parameter for evaluating material scratch performance, is also calculated by the normal load [7, 8]. Moreover, the projected load bearing area plays an important role in scratch hardness calculation [7, 8]. Pelletier et al.'s study demonstrated that the projected load bearing area was mainly related to the scratch indentation

depth, material properties, and indenter shape and tip velocity [8]. Although the indenter size, tip velocity, specimen properties, and external loads all affect the scratch-induced damage severity, only the external loads and tip velocity vary frequently when a patient uses a physical assistant robot. Since the indentation depth is also dependent on the normal load during the abrasion test, the normal load was chosen to examine the effects of external forces on abrasion damage. Therefore, in our study, we first examined the influence of the normal force and tip velocity on the abrasion-induced dummy skin damage. Furthermore, considering the viscoelasticity of skin, stress relaxation plays an important role in the abrasion-induced damage process. Since this parameter is directly related to robot utilization frequency, stress relaxation was also taken into account in the abrasion test. By changing the abrasion times in every trial, we were able to investigate the effects of abrasion frequency. In total, seven different abrasion conditions were tested in our experiments, the details of which are shown in Table 1, where the abrasion frequency refers to the abrasion times in every trial.

4 Results and Discussion

4.1 Abrasion-Induced Damage on Dummy Skin

After several times of abrasion were conducted on the dummy skin, a white wrinkle appeared on its surface, which was the position first contacted by cuff edge. Figure 4 illustrates the stable appearance of the wrinkle, and Fig. 5 provides more detailed information using FESEM. If a relatively small number of times of abrasion were conducted on the dummy skin, this wrinkle disappeared within 1 min after the cuff model left the skin surface. However, the wrinkle's disappearance became slower with increasing abrasion times. According to our experimental observations, if the length of this wrinkle is maintained at greater than or equal to 10 mm during the interval between two continuous trial times, its disappearance will be sufficiently slow and its length almost stable. Therefore, when the wrinkle length was greater than or equal to 10 mm before beginning the next trial, the abrasion times already conducted were recorded and regarded as a criterion for evaluating the abrasion condition hazards.

Fig. 4 Surface appearance of dummy skin after abrasion

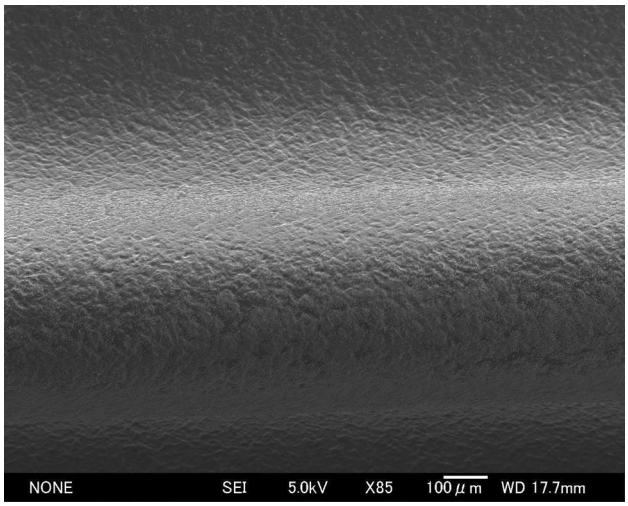

Fig. 5 Scanning electron micrograph of surface appearance of dummy skin after abrasion tests

4.2 Variation of Normal Force and Tangential Force During One Abrasion Time

Under condition 1 of Table 1, the normal and tangential forces measured during one abrasion time were combined into Fig. 6. All the data were processed with a 50^{th}-order low-pass filter with a cutoff frequency of 1 Hz, while the first 50 were deleted to ensure accuracy. It can be seen from Fig. 6 that the entire process can be separated into four stages. In the first stage, the tangential force gradually increases, while the normal force remains relatively stable.

Table 1 Tested abrasion conditions

Order of condition	1	2	3	4	5	6	7
Indentation depth (mm)	3	2	1	2	2	2	2
Tip velocity (mm/s)	2.7	2.7	2.7	5.4	1.35	2.7	2.7
Abrasion frequency (abrasion times/trial)	1	1	1	1	1	2	4

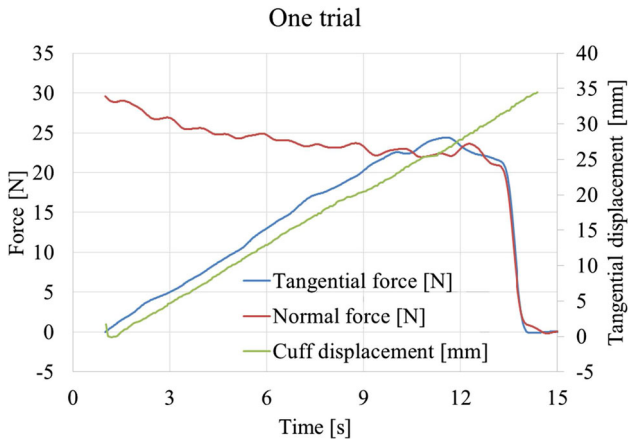

Fig. 6 Normal and tangential force in one abrasion time under condition 1

Accompanied with the cuff tangential displacement in the abrasion direction, the increasing tangential force appears to be caused by the increasing piled-up dummy skin in front of the cuff edge, as shown in Fig. 7. At the end of the first stage, a new, shorter stage appears, in which both the normal force and the ratio between the normal and tangential forces (friction coefficient) remain relatively stable. Thereafter, both the normal and tangential forces begin to decrease sharply and finally become zero after the cuff leaves the skin surface entirely.

4.3 Variation of Normal Force and Tangential Force During One Test

To identify the variation in the normal and tangential forces with increasing abrasion times, a relatively stable characteristic within one abrasion time is necessary to enable location of the same point in every abrasion. As per the phenomenon described in the previous section, the ratio between the normal and tangential forces remains relatively stable in the second stage. Therefore, the highest tangential force was selected from the second stage in one abrasion time, and the ratio between this value and its corresponding normal force was calculated and regarded as the characteristic point of one abrasion time. An entire test consisted of a group of repetitive trials, and one trial was repeated under a fixed condition until a stable wrinkle was generated on the dummy skin surface. The characteristic points for all abrasion times were calculated, and two out of three points were selected for comparison with the first trial.

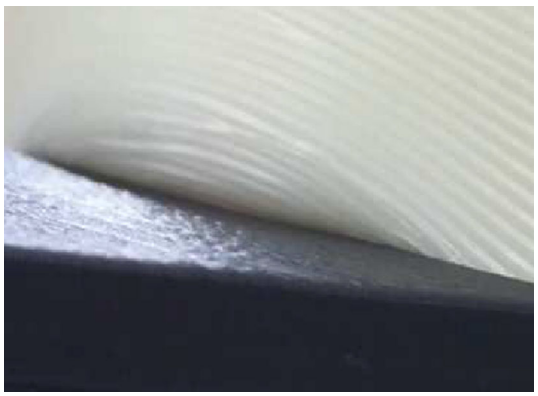

Fig. 7 Dummy skin deformation during abrasion test

4.3.1 *Statistical Analysis*

Statistically significant differences between measurements were determined according to a post hoc one-way variance analysis, which was conducted using the Tukey–Kramer method. The null hypothesis was applied to determine whether the normalized mean ratio value was statistically different from the first abrasion time for different abrasion times. The null hypothesis was rejected for $p < 0.01$ [significance level $\alpha = 0.01$]. Trends were determined by considering the number of measurements [$n = 6$] and statistically significant differences [$p < 0.01$]. The results of the ratio comparison for the six tests are shown in Fig. 8, where the error bars represent the standard deviation above and below the corresponding mean value.

4.3.2 *Variance of the Tangential/Normal Force Ratio*

During one test time, the ratio between the tangential and normal forces decreased gradually until the end of the test. Small fluctuations were also determined during this process; however, after five abrasion times, the ratio decreased significantly, and the decreasing trend became more remarkable with increasing abrasion times. To obtain

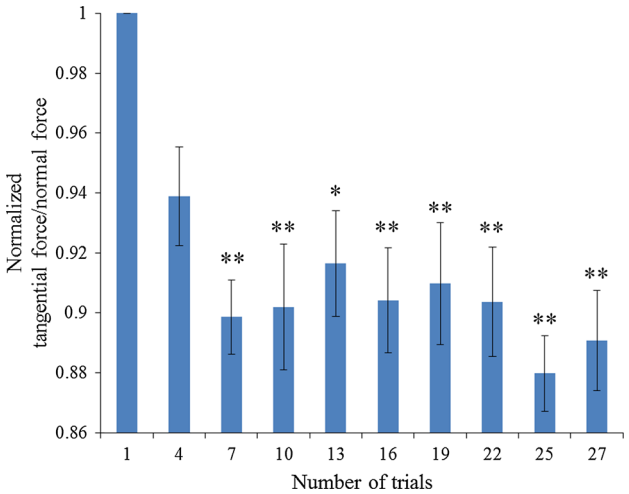

Fig. 8 Comparison of ratio between normal and tangential forces during entire abrasion test

further details for the decreasing process, a similar variance analysis was specifically conducted for the first 11 abrasion times in the six tests, the result of which is shown in Fig. 9. In this case, it can be seen more clearly that after seven abrasion times, the ratio decreases significantly, and the trend becomes more remarkable with increasing abrasion times. The variances of the normal and tangential forces during the 11 abrasion times are also compared in Fig. 10. The normal force exhibited no distinct varying tendency with increasing abrasion times, while the tangential force and the ratio between the forces gradually decreased.

A similar varying tendency was observed for the friction coefficient in the previous scratch study using porcine skin [10]. Fluctuations in the friction coefficient were regarded as sequences of adhesive failure of the skin's stratum corneum layer in Jee et al.'s investigation [10]. The adhesive failure was also demonstrated as the main failure mode in the previous friction blister study conducted on a skin simulant model [16]. Therefore, the significant decrease in the ratio between the tangential and normal forces was considered to be caused by the adhesive delamination of the dummy skin superficial layer.

Since the friction force per unit area typically remains constant, we conclude that the decreasing tendency of the tangential force is caused by a decreased net contact area between the cuff model and dummy skin. As shown in Fig. 4, the skin superficial layer delamination will gradually generate wrinkles on the dummy skin surface. Considering that the decreasing tendency appears when the dummy skin is irreversibly damaged, it is likely that the skin superficial layer delamination, which generates wrinkles on the surface, simultaneously causes a decrease in contact area and declining ratio between the tangential and normal forces.

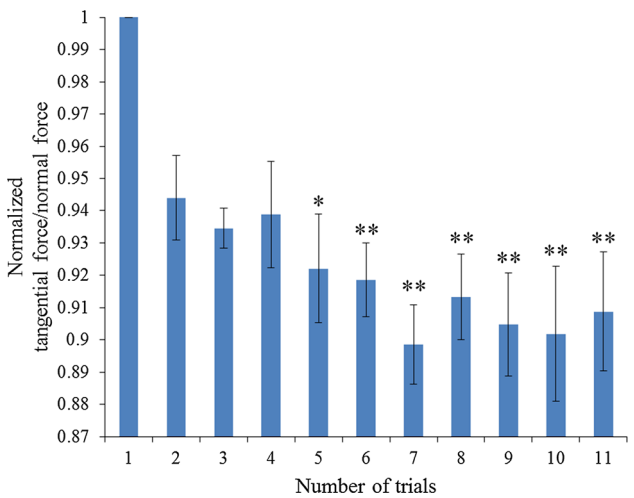

Fig. 9 Comparison of ratio between normal and tangential forces during the first 11 trials

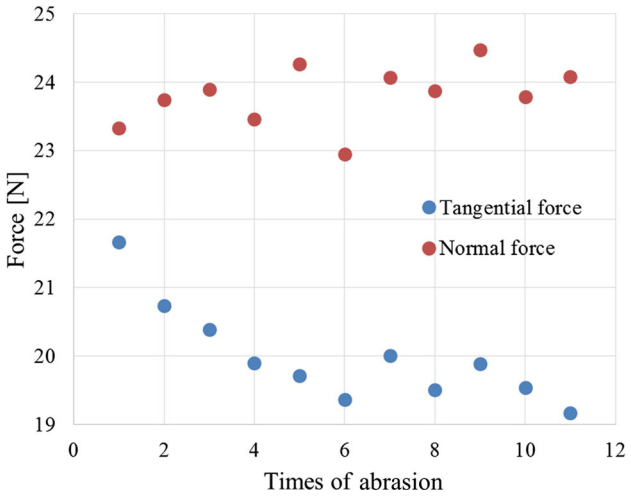

Fig. 10 Comparison of maximum tangential force and its corresponding normal force for each trial in the first 11 repetitions

4.3.3 Skin Surface Morphology Around the Significantly Decreasing Point

By comparing the skin surface morphologies for different abrasion times, as shown in Fig. 11, it can be seen that an obvious damage dot appears after five abrasion times. This dot indicates irreversible damage generated on the skin surface, the separation at the superficial layer–skin substrate interface. Because five abrasion times can also cause a significant decrease in the ratio between the tangential and normal forces, this can be regarded as a warning of irreversible skin abrasion damage.

4.4 Influences of Abrasion Times on the Adhesion Work of the Dummy Skin Superficial Layer

After we finished two abrasion tests, the two pieces of dummy skin samples with a wrinkle on it were cut into two strips 10 mm wide. For each skin sample, one more strip was also taken as a control sample from the area where no contact happens between the cuff and the skin during the abrasion test. The four strips were preprocessed by the method described in Sect. 3.1 and peeled by the tension and compression testing machine. The appearance of the sample before adhesion test is shown in Fig. 12. The peeling force and the displacement recorded during the peeling test are plotted in Fig. 13.

As shown in Fig. 13, the force for peeling the superficial film of the samples after abrasion is much lower than that of the samples without abrasion. When it is around the wrinkle position, i.e., the displacement is between 0 and 5 mm, the peeling force significantly decreases once, which indicates that the abrasion damage appearing as the

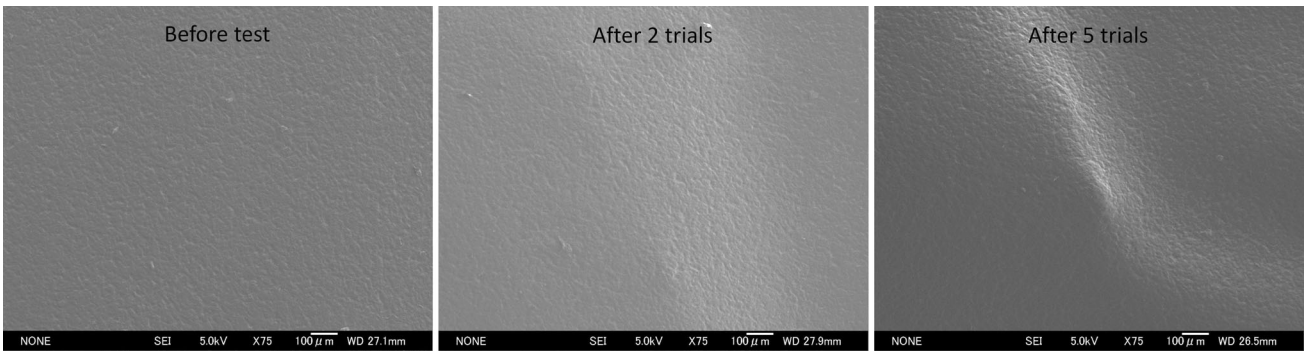

Fig. 11 Scanning electron micrographs of dummy skin surface morphologies for different abrasion times

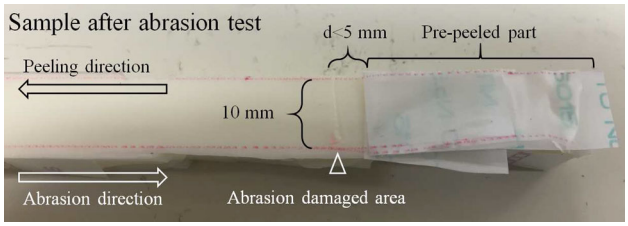

Fig. 12 Preprocessed sample for adhesion test

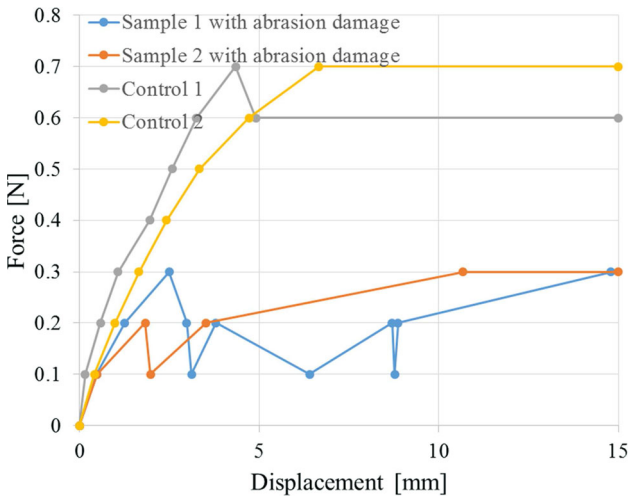

Fig. 13 Peeling force and displacement during adhesion test for skin samples after entire abrasion tests

adhesive delamination apparently reduces the adhesion of the dummy skin superficial film.

In order to investigate the detailed relationship between the abrasion times and the remained adhesion, the superficial film adhesion of the dummy skin samples was further examined after three different times of abrasion. The peeling force and the displacement recorded in the tests are summarized in Fig. 14. It also appears that the more times of abrasion the dummy skin suffers, the less force is needed to peel the skin superficial layer.

As demonstrated in Wei's previous study [27], the work of adhesion (energy per unit area) W can be calculated with

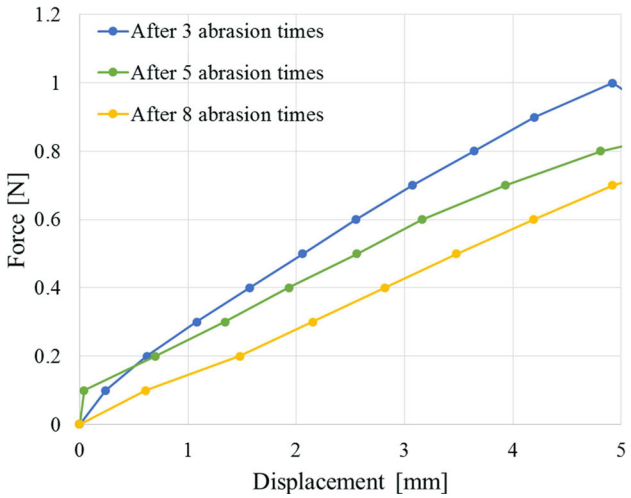

Fig. 14 Peeling force and displacement during adhesion test for skin samples after different times of abrasion

the peel force per unit width of the film F and the peel angel ϕ

$$W \approx F(1 - \cos\phi) \quad (1)$$

It should be noted that the above calculation was started from the point when the pre-peeled part was sufficiently stretched in each of the adhesion test to exclude the elastic energy as much as possible. The calculated work of adhesion for different samples is summarized in Table 2. The relationship between the adhesion test results and the possible analytical model of friction trauma mechanics will be discussed later in Sect. 4.5.

Table 2 Work of adhesion after different times of abrasion

Times of abrasion	3	5	8
Work of adhesion (kJ/m^2)	8.8	5.9	2.9

4.5 Influences of Different Parameters on the Dummy Skin Abrasion Damage

To confirm the effects of the various physical parameters on abrasion-induced damage, a series of experiments were conducted using three different sets of conditions, normal load levels, abrasion velocities, and abrasion frequencies. Figure 15 shows the variances of the normal and tangential forces in one abrasion time under different conditions.

The different indentation depths applied in the abrasion tests resulted in different normal loads exerted on the dummy skin. Figure 16 shows the normal force values at the maximum tangential force point (TFmax) for the different depths. Because the dummy leg stood stably during the test, the time of the four stages increases with an increased indentation depth and normal force. For the series of tests conducted using different abrasion velocities, as shown in Fig. 15a, the time of one abrasion motion decreases with increased velocity, which is caused by the constant abrasion distance. In contrast, the normal force level barely changes among the tests with the three different velocities and abrasion frequencies, which are shown in Fig. 15b, c.

For the tests conducted under different conditions, three figures were drawn to show how the respective physical parameters affected the abrasion times required to generate a wrinkle with a stable length (that is, abrasion times until the test end), which are summarized in Fig. 17. A post hoc one-way variance analysis was also conducted to compare the difference influences. The analysis method is similar to the one described in Sect. 4.3.1, and the results are shown in the same figure.

From Fig. 17, the abrasion frequency appears to be insignificant to the abrasion damage inside the tested range. The one-way variance analysis conducted to determine the effect of abrasion frequency on abrasion damage severity provided a similar result, namely that the influence of the tested abrasion frequencies showed few theoretically significant differences. In contrast, the severity of abrasion damage increases with the increase in the indentation depth and normal load and decreases with the increase in the tip velocity when the abrasion distance maintains constant.

As claimed in Blees et al.'s study [28], the critical load L_{crit} of debonding the sol–gel film from the polypropylene substrate is proportional to the square root of the work of adhesion W

$$L_{\text{crit}} = \frac{\pi}{4}\frac{\tau_{\text{crit}} d_{\text{crit}}^2}{\mu_{\text{crit}}}, \tag{2}$$

since the work of adhesion can be calculated as

$$W = \frac{\tau_{\text{crit}}^2}{2E} t, \tag{3}$$

where $d_{\text{crit}}, \mu_{\text{crit}}, \tau_{\text{crit}}$ are the critical width of scratch damage, friction coefficient and shear stress, and E and t are the Young's modulus and thickness of the coating film.

Since d_{crit} almost maintained constant under the same condition, $L_{\text{crit}}\mu_{\text{crit}}$ should be proportional to the square root of the work of adhesion, i.e., the tangential load should be proportional to the square root of the work of adhesion. If the abrasion times can be verified to be inversely proportional to the corresponding square root of the work of adhesion, the tangential load should also be inversely proportional to the abrasion times for generating a certain degree of abrasion damage.

Based on the results in Table 2, the relationship between the abrasion times (AT) and the square root of the corresponding adhesion work W yields a least-squares fit of the form

$$\sqrt{W} = 10.44\ AT^{-1} \tag{4}$$

The R^2 value of the fit is 0.78, which indicates that the square root of the adhesion work is reasonably considered to be inversely proportional to the abrasion times.

According to the above hypothesis, the relationship between the tangential load and the abrasion times until the test end is exhibited with the trend lines in Fig. 18, where x is the number of the abrasion times until the test end, and y is the maximum tangential force in one time of abrasion. The R^2 value of the trend line is also shown in the same figure.

The relative higher R^2 values shown in Fig. 18 confirm the consistency between the analytical model established with our experimental system and the conventional scratch mechanical model. Therefore, the influences of the significant parameter on the skin abrasion damage can be determined with the analytical model, and our method is verified to be feasible for evaluating the skin–cuff contact state and estimating the severity of abrasion injury.

5 Conclusions and Future Work

In this study, we have established a novel method for evaluating contact states between a physical assistant robot's cuff and human skin. To realize efficient evaluation, a simplified cuff model was firstly designed to exert a load on the contact surface during the abrasion test. The variances of the normal force, tangential force, and friction coefficient were observed during the abrasion test, and a significant clue for irreversible abrasion damage was determined by comparing the varying tendencies of the friction coefficient. Based on the abrasion damage

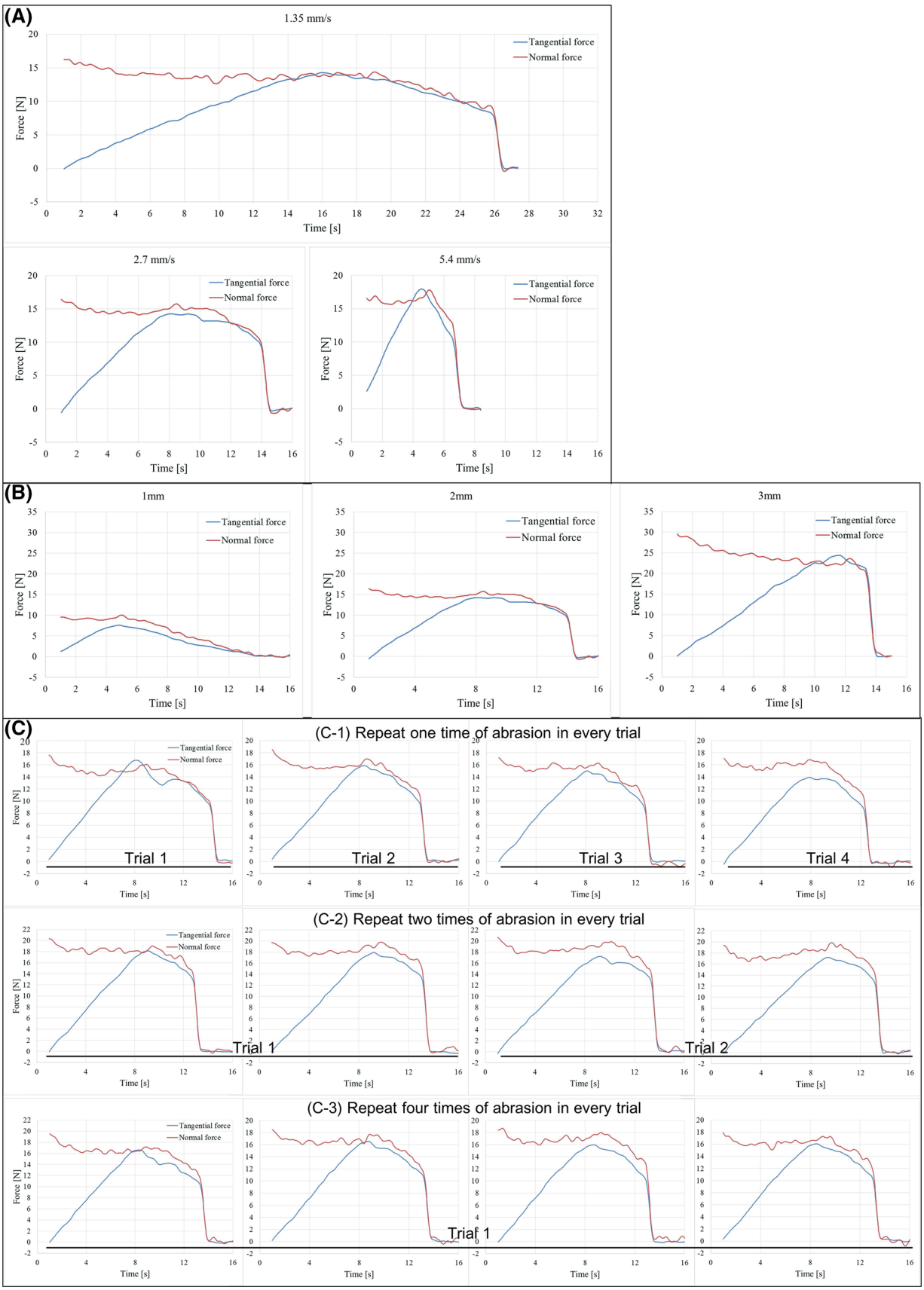
(A)
1.35 mm/s
2.7 mm/s
5.4 mm/s
Tangential force
Normal force
Force [N]
Time [s]
(B)
1mm
2mm
3mm
(C)
(C-1) Repeat one time of abrasion in every trial
Trial 1
Trial 2
Trial 3
Trial 4
(C-2) Repeat two times of abrasion in every trial
Trial 1
Trial 2
(C-3) Repeat four times of abrasion in every trial
Trial 1

◀**Fig. 15** Normal and tangential forces in one abrasion time with different **a** tip velocities (conditions 2, 4, and 5 in Table 1), **b** indentation depths (conditions 1, 2, and 3 in Table 1) or **c** abrasion frequencies (conditions 2, 6 and 7 in Table 1)

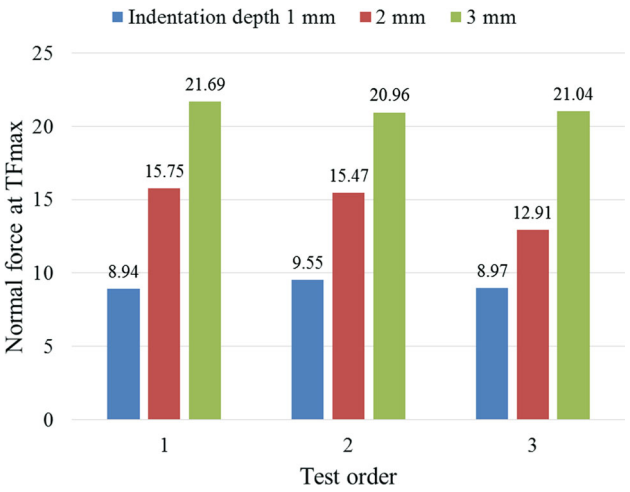

Fig. 16 Comparison of normal force values at TFmax during one abrasion time with different indentation depths

mechanism and actual use of physical assistant robots, three physical factors were regarded as having the most significant effect on skin abrasion trauma. The different influences of these physical factors on the abrasion damage were subsequently determined with abrasion times in an analytical model, which provides a feasible way for the evaluation of human skin–robot cuff contact state and estimation of abrasion damage severity.

In the future, we would like to verify that the clue of irreversible dummy skin abrasion damage can also act as a warning for initial human skin abrasion trauma. The evaluation method for the skin–cuff contact condition will be further improved by matching the dummy skin contact mechanics with those of in vitro skin samples, so that the abrasion times can be applied as a reliable criterion in the evaluation directly contributing to the safety validation of physical assistant robots.

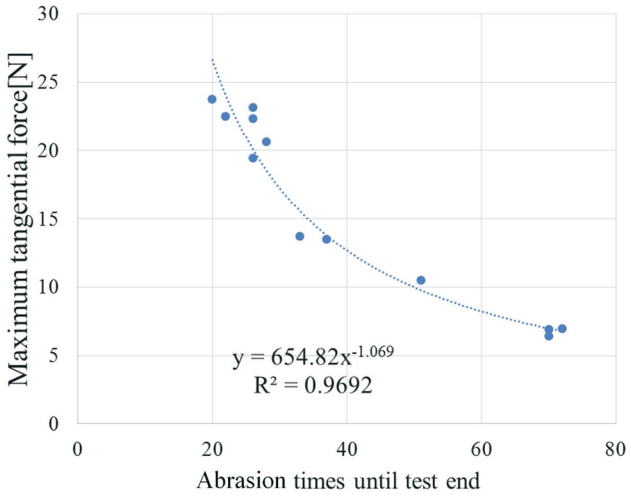

Fig. 18 Relationship between tangential load and abrasion times until test end

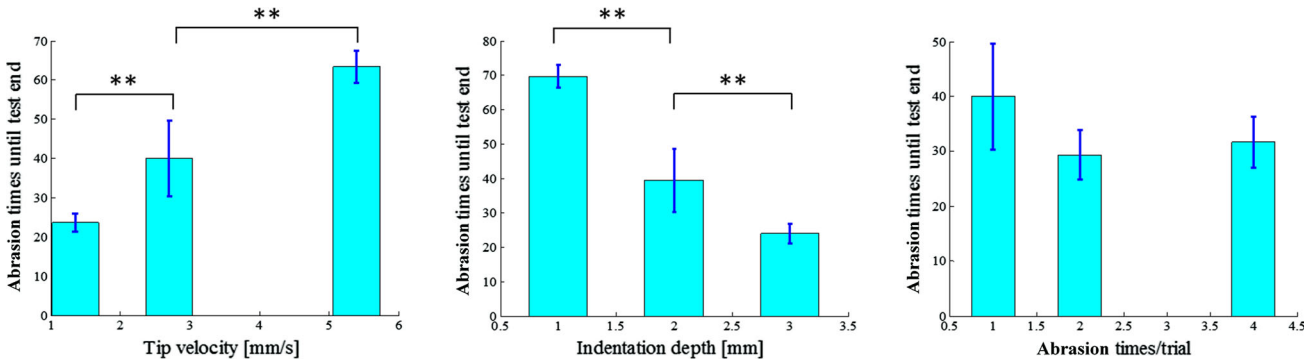

Fig. 17 Influences of different parameters on abrasion times until test end

Acknowledgements This work was supported by AMED (Japan Agency for Medical Research and Development). The authors would also like to thank Mr. Akihiro Kato, Nagoya University, and Mr. Xudong Hao, University of Michigan, for their technical support for cuff–dummy skin interactive force data collection.

References

1. Stubblefield, H.: Cut and scratches. Healthline. http://www.healthline.com/health/cuts-scratches#Overview1 (2016). Accessed 19 July 2016
2. Blahd, W.H., Husney, A., Gabica J.M.: Scrapes. HealthLinkBC. https://www.healthlinkbc.ca/health-topics/srape (2016). Accessed 27 May 2016
3. Dunkin, C.S., Pleat, J.M., Gillespie, P.H., Tyler, M.P., Roberts, A.H., McGrouther, D.A.: Scarring occurs at a critical depth of skin injury: precise measurement in a graduated dermal scratch in human volunteers. Plast. Reconstr. Surg. **119**(6), 1722–1732 (2007)
4. Kyouko, O.: Current status of the introduction of lower extremity functional training with the robot suit hal in our hospital. Jpn. J. Press. Ulcers **16**(3), 289 (2014)
5. Sanders, J.E., Goldstein, B.S., Leotta, D.F.: Skin response to mechanical stress: adaptation rather than breakdown-a review of the literature. J. Rehabil. Res. Dev. **32**(3), 214–226 (1995)
6. Jiang, H., Browning, R., Sue, H.J.: Understanding of scratch-induced damage mechanisms in polymers. Polymer **50**(16), 4056–4065 (2009)
7. Kurkcu, P., Andena, L., Pavan, A.: An experimental investigation of the scratch behaviour of polymers: 1. Influence of rate-dependent bulk mechanical properties. Wear **290**, 86–93 (2012)
8. Pelletier, H., Mendibide, C., Riche, A.: Mechanical characterization of polymeric films using depth-sensing instrument: correlation between viscoelastic-plastic properties and scratch resistance. Prog. Org. Coat. **62**(2), 162–178 (2008)
9. Giannakopoulos, A., Lindley, T., Suresh, S., Chenut, C.: Similarities of stress concentrations in contact at round punches and fatigue at notches: implications to fretting fatigue crack initiation. Fatigue Fract. Eng. Mater. Struct. **23**(7), 561–572 (2000)
10. Jee, T., Komvopoulos, K.: In vitro investigation of skin damage due to microscale shearing. J. Biomed. Mater. Res. Part A **102**(11), 4078–4086 (2014)
11. Naylor, P.F.D.: Experimental friction blisters. Br. J. Dermatol. **67**(10), 327–342 (1955)
12. Mao, X., Yamada, Y., Akiyama, Y., Okamoto, S., Yoshida, K.: Development of a novel test method for skin safety verification of physical assistant robots. In: IEEE international conference on rehabilitation robotics (ICORR), 2015, pp. 319–324. IEEE (2015)
13. Xing, M., Pan, N., Zhong, W., Maibach, H.: Skin friction blistering: computer model. Skin Res. Technol. **13**(3), 310–316 (2007)
14. Guerra, C., Schwartz, C.: Development of a synthetic skin simulant platform for the investigation of dermal blistering mechanics. Tribol. Lett. **44**(2), 223 (2011)
15. Guerra, C., Schwartz, C.: Investigation of the influence of textiles and surface treatments on blistering using a novel simulant. Skin Res. Technol. **18**(1), 94–100 (2012)
16. Chimata, G.P., Schwartz, C.J.: Investigation of the effect of the normal load on the incidence of friction blisters in a skin-simulant model. Proc. Inst. Mech. Eng. Part J J. Eng. Tribol. **229**(3), 266–272 (2015)
17. Aso, M., Yamada, Y., Yoshida, K., Akiyama, Y., Ito, Y.: Evaluation of the mechanical characteristics of human thighs for developing complex dummy tissues. In: IEEE international conference on robotics and biomimetics (ROBIO), 2013, pp. 1450–1455. IEEE (2013)
18. Naylor, P.F.D.: The skin surface and friction. Br. J. Dermatol. **67**(7), 239–8 (1955)
19. Tang, H., Martin, D.C.: Near-surface deformation under scratches in polypropylene blends Part I microscopic characterization of deformation. J. Mater. Sci. **38**(4), 803–815 (2003)
20. Knapik, J.J., Reynolds, K.L., Duplantis, K.L., Jones, B.H.: Friction blisters. Sports Med. **20**(3), 136–147 (1995)
21. Goldstein, B., Sanders, J.: Skin response to repetitive mechanical stress: a new experimental model in pig. Arch. Phys. Med. Rehabil. **79**(3), 265–272 (1998)
22. Adams, M., Briscoe, B., Johnson, S.: Friction and lubrication of human skin. Tribol. Lett. **26**(3), 239–253 (2007)
23. Kwiatkowska, M., Franklin, S., Hendriks, C., Kwiatkowski, K.: Friction and deformation behaviour of human skin. Wear **267**(5), 1264–1273 (2009)
24. Swindle, M.M.: Porcine integumentary system models: Part 1 - Dermal toxicology. Sinclair Research Center. http://www.sinclairresearch.com/Downloads/TechnicalBulletins/Porcine/20Integumentary/20System/20Model-Part/201.pdf (2008). Accessed 2008
25. Dai, T., Tegos, G.P., Zhiyentayev, T., Mylonakis, E., Hamblin, M.R.: Photodynamic therapy for methicillin-resistant staphylococcus aureus infection in a mouse skin abrasion model. Lasers Surg. Med. **42**(1), 38 (2010)
26. Bhagavathula, N., Warner, R.L., DaSilva, M., McClintock, S.D., Barron, A., Aslam, M.N., Johnson, K.J., Varani, J.: A combination of curcumin and ginger extract improves abrasion wound healing in corticosteroid-impaired hairless rat skin. Wound Repair Regen. **17**(3), 360–366 (2009)
27. Wei, Y., Hutchinson, J.W.: Interface strength, work of adhesion and plasticity in the peel test. Int. J. Fract. **93**(1), 315–333 (1998)
28. Blees, M.H., Winkelman, G.B., Balkenende, A.R., Den Toonder, J.M.J.: The effect of friction on scratch adhesion testing: application to a sol–gel coating on polypropylene. Thin Solid Films **359**(1), 1–13 (2000)